Revealing the Bound Nucleon 3D Partonic Structure through Incoherent Deeply Virtual Compton Scattering off ^{4}He

M. Hattawy,[1,2] N.A. Baltzell,[1,3] R. Dupré,[2,1] K. Hafidi,[1] and S. Stepanyan[3]
(The CLAS Collaboration)
[1] *Argonne National Laboratory, Argonne, Illinois 60439*
[2] *Institut de Physique Nucléaire, CNRS/IN2P3 and Université Paris Sud, 91406 Orsay, France*
[3] *Thomas Jefferson National Accelerator Facility, Newport News, Virginia 23606*
(Dated: February 14, 2018)

We report on the beam-spin asymmetries associated with incoherent deeply virtual Compton scattering off ^{4}He in the valence quark region. The data have been accumulated using a 6 GeV longitudinally-polarized electron beam incident on a pressurized ^{4}He gaseous target placed in front of the CLAS spectrometer in Hall-B at Thomas Jefferson National Accelerator Facility. The baseline detection sub-systems of CLAS detected the scattered electrons and the recoil protons, while the final-state real photons are detected by a supplementary electromagnetic calorimeter at very forward angles. The measured beam-spin asymmetries on bound-protons exhibit a suppression compared to those on free proton, indicating possible medium modifications on the nucleon's quark distributions and opening new opportunities to explore the origin of the EMC effect within the framework of the generalized parton distributions.

PACS numbers: Valid PACS appear here

Electromagnetic probes have played a major role in advancing our knowledge about the structure of nucleons, which are the origin of almost all the Universe visible matter. While the elastic lepton-nucleon measurements have taught us about the spatial charge and magnetization distributions [1, 2], the deep-inelastic scattering (DIS) experiments have uncovered the features of momentum sharing between the constituents partons, i.e., quarks and gluons [3, 4]. With nuclear targets, the DIS measurements have revealed the fact that the distribution of quarks in a fast moving nucleus is not a simple convolution of their distributions within nucleons, known as the "EMC effect"[5] (for reviews on the extensive investigations, see [6–12]).

A wealth of information on the structure of matter lies in the correlations between the momentum and spatial degrees of freedom of the partons. These correlations are set to be revealed through deeply virtual Compton scattering (DVCS), i.e., the hard exclusive leptoproduction of a real photon, which provide access to a three-dimensional imaging of partons within the generalized parton distributions (GPDs) framework [13–17]. The free proton DVCS measurement has been the focus of a worldwide effort [18–29] involving several accelerator facilities such as Jefferson Lab (JLab), HERA and CERN. Combining these measurements has enabled the first tomography extraction of the free proton [31]. New groundbreaking measurements of exclusive DVCS from the ^{4}He nucleus are a critical step towards providing similar 3D pictures of the quark structure of the nucleus as a whole, via the coherent channel [32], and provide a new approach to understanding the partonic modifications of the bound nucleons via the incoherent DVCS channel [33–35]. The ^{4}He nucleus is an ideal experimental target for these purposes as it has only one chiral-even GPD that parametrizes its partonic structure, is characterized by a strong binding energy, and has a relatively high nuclear core density. The inclusive scattering off ^{4}He has shown a large EMC effect [30], making this nucleus a golden target for investigating the medium partonic modifications.

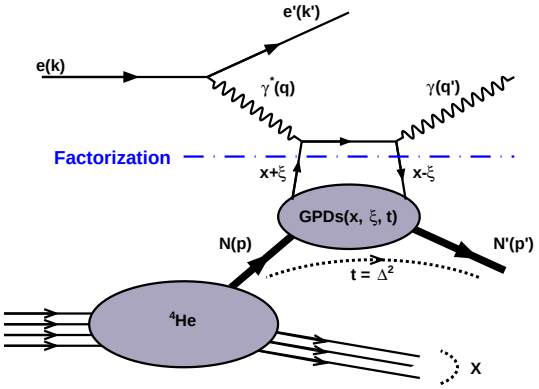

FIG. 1: Representation of the leading-order, twist-2, handbag diagram of the incoherent DVCS process off ^{4}He, where the four-vectors of the electrons, photons, and protons are denoted by k/k', q/q', and p/p', respectively. $x+\xi$ is the nucleons longitudinal momentum fraction carried by the struck quark, 2ξ is the longitudinal momentum fraction of the momentum transfer Δ $(= p - p')$, and t $(= \Delta^2)$ is the squared momentum transfer between the initial and the final state nucleon.

FIG. 1 illustrates a schematic representation of the leading-twist handbag diagram for the incoherent DVCS off ^{4}He. In the Bjorken region, i.e, large virtual photon four-momentum squared $(Q^2 = -(k-k')^2)$, and at small

invariant momentum transfer (t), the DVCS handbag diagram can be factorized, leaving the non-perturbative structure of the nucleon to be parametrized in terms of four chirally-even GPDs: H, E, $\widetilde{H}$, and $\widetilde{E}$, representing the four helicity-spin combinations of the quark-nucleon states [36, 37].

In this Letter, we present the beam-spin asymmetries associated with the photon electroproduction on bound-proton off ^{4}He. While the experimentally measured cross section amplitude is the sum of the DVCS, BH (i.e., the final state real photon is emitted by the incident or the scattered electron), and their interference, the beam-spin asymmetry observable is sensitive to the amplitudes that contain information on the GPDs, i.e., DVCS and interference amplitudes. The beam-spin asymmetry observable is measurable using a polarized lepton beam on unpolarized target (U) and defined in terms of the cross sections as

$$A_{LU} = \frac{d^5\sigma^+ - d^5\sigma^-}{d^5\sigma^+ + d^5\sigma^-}. \quad (1)$$

where $d^5\sigma^+(d^5\sigma^-)$ is the photon electroproduction differential cross section for a positive (negative) beam helicity.

Following the cross section decomposition suggested by [38], the different amplitudes can be expressed in terms of Fourier coefficients associated with ϕ-harmonics, where ϕ is the angle between the leptonic and the hadronic planes of the reaction. At leading-twist, the beam-spin asymmetry can be simplified as

$$A_{LU}(\phi) = \frac{a_0 \sin(\phi)}{1 + a_1 \cos(\phi) + a_2 \cos(2\phi)} \quad (2)$$

with the parameters $a_{0,1,2}$ are combinations of the above mentioned Fourier coefficients. The first sine harmonic of the beam-spin asymmetry is dominant and proportional to the following combination of Compton form factors (CFF) [39]

$$A_{LU}^{\sin\phi} \propto \mathrm{Im}(F_1\mathcal{H} - \frac{t}{4M^2}F_2\mathcal{E} + \frac{x_B}{2}(F_1+F_2)\tilde{\mathcal{H}}) \quad (3)$$

where F_1 and F_2 are the Dirac and Pauli form factors with x_B as the Bjorken scaling variable. The real and the imaginary parts of the CFF $\mathcal{H}$ are corresponding to the GPD H by

$$\Re(\mathcal{H}) = \mathcal{P}\int_0^1 dx[H(x,\xi,t) - H(-x,\xi,t)]\, C^+(x,\xi) \quad (4)$$

$$\Im(\mathcal{H}) = -\pi[H(\xi,\xi,t) - H(-\xi,\xi,t)], \quad (5)$$

with $\mathcal{P}$ is the Cauchy principal value integral and C^+ is a coefficient function defined as $(1/(x-\xi)+1/(x+\xi))$ with ξ being related to x_B by $\xi \approx \frac{x_B}{2-x_B}$. Similar expressions apply for the GPDs E, $\widetilde{H}$, and $\widetilde{E}$.

The experiment (E08-024 [40]) took place in Hall-B of Jefferson Lab using the nearly 100% duty factor, longitudinally-polarized electron beam (83% polarization) from the Continuous Electron Beam Accelerator Facility (CEBAF) accelerator at its full energy of 6.064 GeV. The data were accumulated over 40 days using a 6-atm-pressure, 292-mm-long, and 6-mm-diameter gaseous ^{4}He target centered at 64 cm upstream of the CEBAF Large Acceptance Spectrometer (CLAS) center. For similar DVCS experiments on free-proton target [24, 29], the CLAS baseline design [41] is supplemented with an inner calorimeter (IC) and a solenoid. The IC extends the photon detection acceptance of CLAS, which was originally from 15° to 45°, to polar angles as low as 4°. As the coherent DVCS off ^{4}He, where the nucleus remain intact, was one of the proposed measurements of our experiment and since CLAS cannot detect such low-energy recoil nuclei, we built a small radial time projection chamber (RTPC) around the target cell. (See [42] for a detailed description of the RTPC and its performances and [32] for the coherent DVCS measurements). In this setup, the 5-Tesla solenoid (that surrounds the target and the RTPC) enabled the detection of the low-energy charged ions in the RTPC and prevented the high-rate low-energy Møller electrons from reaching CLAS sub-detectors by guiding these electrons towards a heavy shield placed around the beam line.

Incoherent DVCS events were selected if an electron, a proton, and at least one photon were detected in the final state. Electrons were identified by having appropriate deposited energy in the electromagnetic calorimeter and proper light yield in the Cherenkov counters in addition to having a negative track-curvature in the drift chambers that corresponds to a momentum greater than 800 MeV. The protons were distinguished from other positive particles by timing cuts established using the time-of-flight measured by the scintillators and the reconstructed track information from the drift chambers. Also, the selected proton was required to be originating from the electron's vertex by applying a vertex matching cut. The photons were detected in either the IC or the CLAS electromagnetic calorimeter. All the signals within IC fiducial region were assumed to be photons, while a timing cut is used to clean the EC photons from neutrons. Note that even though the DVCS reaction has only one real photon in the final state, events with more than one good photon are not discarded at this stage. It was observed by the DVCS exclusivity cuts, discussed below, that most of these photons are soft ones produced in random coincidence. In the following selection stage, the most energetic photon is considered as the DVCS photon candidate (see [43] for additional details on the particles identification).

Further requirements were applied to clean the identified initial set of incoherent DVCS events from backgrounds and other channels. Events were selected with Q^2 greater the 1 GeV^2 to ensure that the interaction occurs at the partonic level and the applicability of the factorization on the DVCS handbag diagram, $\gamma^* p$ invariant mass (W) greater than 2 GeV to avoid the nucleon region

of excitation to resonances, and the transferred momentum squared to the recoil proton has to be greater than a minimum value defined by the kinematics of the beam and the scattered electron ($-t > -t_{min}$). Then, the exclusivity of the incoherent DVCS events was ensured by imposing constraints on the kinematical variables resulting from conserving the four-momentum in the reaction $ep \to e'p'\gamma$. These kinematical variables are: the coplanarity angle $\Delta\phi$ between the (γ, γ^*) and (γ^*, p') planes, the missing energy, mass, and transverse momentum of the $e'\gamma$ and $e'p'\gamma$ system, the missing mass squared of the $e'p'$ system, and the angle θ between the measured photon and the missing momentum of the $e'p'$ system. The experimental data for the most relevant exclusivity variables and applied cuts are shown in FIG. 2 (see [43] for additional details). We also rejected events where a π^0 was identified by the invariant mass of two photons. About 30k events passed all these requirements; their kinematic distributions are shown in FIG. 3.

In spite of our selection requirements, two main backgrounds were observed to contaminate our incoherent DVCS sample; accidental coincidences and exclusive π^0 production. For the accidental events, i.e., $e'p'\gamma$ collection with particles originated from different events, their contribution of 6.5% was evaluated by selecting events passing all our cuts but originating from different vertices. Regarding the π^0 contamination, i.e., $ep \to e'p'\pi^0$ events where one of the two photons of the π^0 decay is produced below the energy threshold or outside the detection acceptance, we evaluated this contribution by using data and simulation. From the simulation, we calculated the ratio (R) between the number of π^0 events where the two photons are detected and those that would be mistaken for DVCS ($R = N^{1\gamma}_{sim}/N^{2\gamma}_{sim}$). Then in each kinematical bin and for each beam-helicity state, the π^0-subtracted experimental DVCS events is calculated as $N = N^{ep\to e'p'\gamma}_{exp} - R\ N^{ep\to e'p'\pi^0}_{exp}$, where $N^{ep\to e'p'\gamma}_{exp}$ is the experimentally identified number of $ep \to e'p'\gamma$ and $N^{ep\to e'p'\pi^0}_{exp}$ is the experimentally identified $ep \to e'p'\pi^0$ with the two photons were detected. Depending on the kinematics, we found contaminations of 8%-10%.

It is convenient to use the beam-spin asymmetry as a DVCS observable because the cross sections luminosity normalization and detector efficiencies cancel out in the asymmetry ratio. Experimentally, A_{LU} can be simplified in terms of the reaction yield in each beam-helicity state ($N^{\pm}$) as

$$A_{LU} = \frac{1}{P_B}\frac{N^+ - N^-}{N^+ + N^-}. \qquad (6)$$

where P_B is the longitudinal beam polarization.

Following the model guidance of [39], the GPD H dominants the other three GPDs within the accessible phase-phase of using the 6 GeV electron beam from CEBAF and CLAS spectrometer. Therefore, measuring A_{LU} gives access to the real and imaginary part of the CFF $\mathcal{H}$

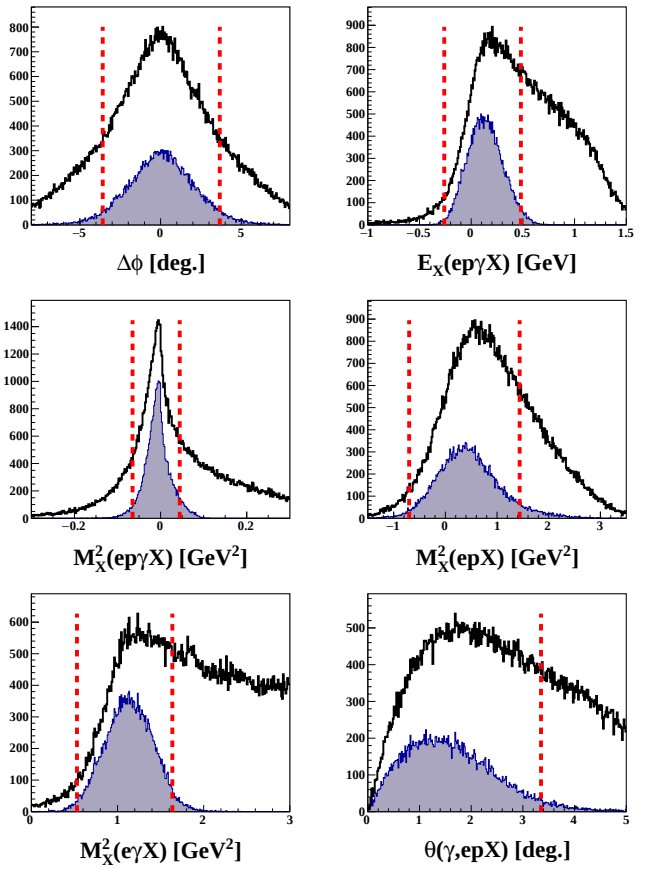

FIG. 2: The incoherent DVCS exclusivity cuts. The black distributions represent the incoherent DVCS events candidate before all the exclusive cuts. The shaded distributions represent the incoherent DVCS events which passed all the exclusivity cuts except the quantity plotted. The vertical red lines represent the applied exclusivity cuts. The distributions from left to right and from top to bottoms are: $\Delta\phi$, missing energy, missing masses squared and the cone angle (θ) between the measured and the calculated photons in the $e'p'$ final-state system.

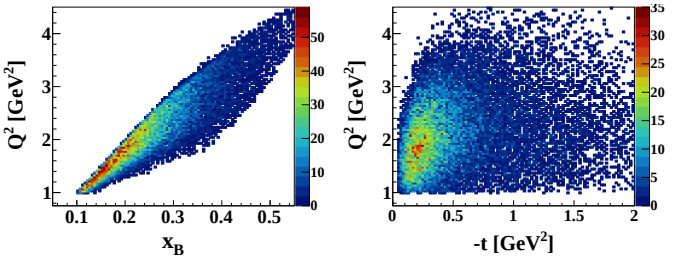

FIG. 3: Incoherent DVCS event distributions for Q^2 as a function of x_B (left) and Q^2 as a function of $-t$ (right) after the exclusivity cuts.

through the parameters a_0, a_1, and a_2 of equation 2. Moreover, the free proton A_{LU} measurements, [24], have shown that the $cos(2\phi)$ term, which is corresponding to the pure DVCS amplitude, is suppressed and compatible

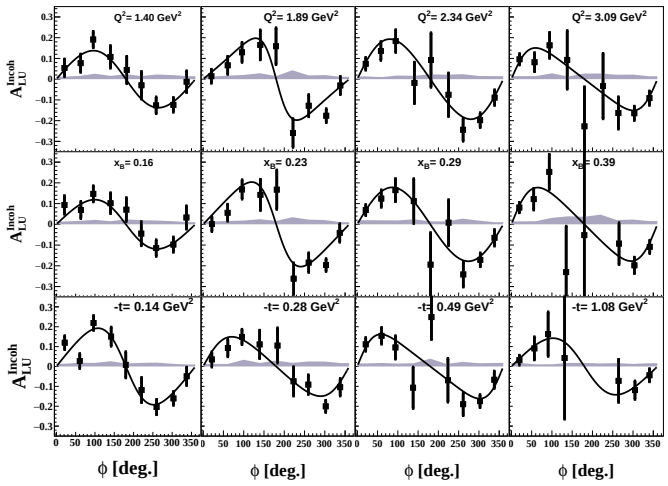

FIG. 4: The incoherent A_{LU} as a function of ϕ. Results are presented for different Q^2 bins (top panel), x_B bins (middle panel), and $-t$ bins (bottom panel). The error bars represent the statistical uncertainties. The gray bands represent the systematic uncertainties, including the normalisation uncertainties. The black curves are the results of our fits with the form $\frac{a_0\ sin(\phi)}{1+a_1\ cos(\phi)}$.

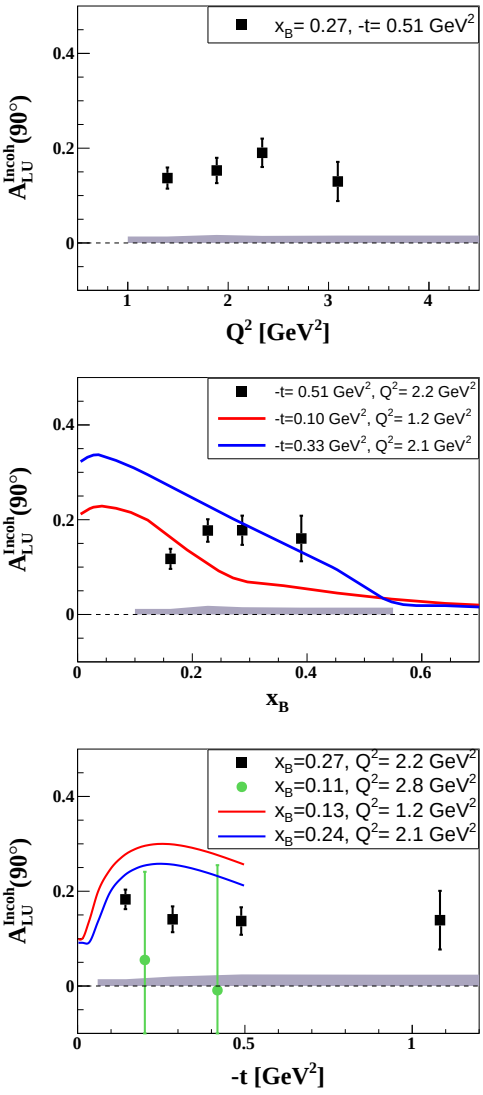

FIG. 5: The Q^2 (top), x_B (middle), and t dependencies (bottom) of the fitted A_{LU} at $\phi = 90°$ (black squares). The error bars represent the statistical uncertainties, while the gray bands represent the systematic uncertainties. On the middle plot: the curves are theoretical calculations from [33]. On the bottom: the green circles are the HERMES $-A_{LU}$ (positron beam was used) inclusive measurements [19], the curves represent theoretical calculations from [33].

with zero.

Due to limited statistics, the data were binned two-dimensionally into 36 bins. That is, four statistically-equivalent bins in each of the kinematical variables (Q^2, x_B, t) were constructed one at a time. Then, each bin is divided into nine bins in the azimuthal angle (ϕ). FIG. 4 presents the measured incoherent A_{LU} as a function of ϕ in bins in Q^2, x_B, and t. The curves on the plots are fits of the approximated form $\frac{a_0\ sin(\phi)}{1+a_1\ cos(\phi)}$. The study of systematic uncertainties showed that the main contributions come from the choice of the DVCS exclusivity cuts (6%) and the large binning size (7%). However, added quadratically, these uncertainties sum up to about 10%, which always remains significantly smaller than the statistical errors.

We present in FIG. 5 the dependence of the fitted A_{LU} signals at $\phi = 90°$ on the kinematical variables Q^2, x_B, and t. Within the given uncertainties, A_{LU} does not indicate a strong dependence on Q^2. The x_B and t dependencies are compared to theoretical calculations performed by S. Liuti and K. Taneja [33]. Their model uses a realistic spectral function and considers off-shell effects. The calculations are carried out at slightly different kinematics than our data but still provide some guidance. The experimental results appear to have smaller asymmetries than the calculations. These differences may arise from nuclear effects which are not taken into account in the model, such as long-range interactions.

In this work we carried out the first step towards measuring the "generalized" EMC effect in order to understand the potential sources of nuclear effects at the partonic level within the GPDs framework. We construct the ratio of A_{LU} for bound protons to that on free proton target measured using similar electron-beam energy and experimental setup. FIG. 6 presents the dependence of the beam-spin asymmetry ratio at $\phi = 90°$ on the kinematical variables Q^2, x_B, and t. The free proton asymmetries were interpolated from the published results [24].

The A_{LU} ratios show a 20%-40% suppression in the bound protons compared to the free protons. These measurements disagree with the enhancement predicted by the on-shell calculations that use the medium modi-

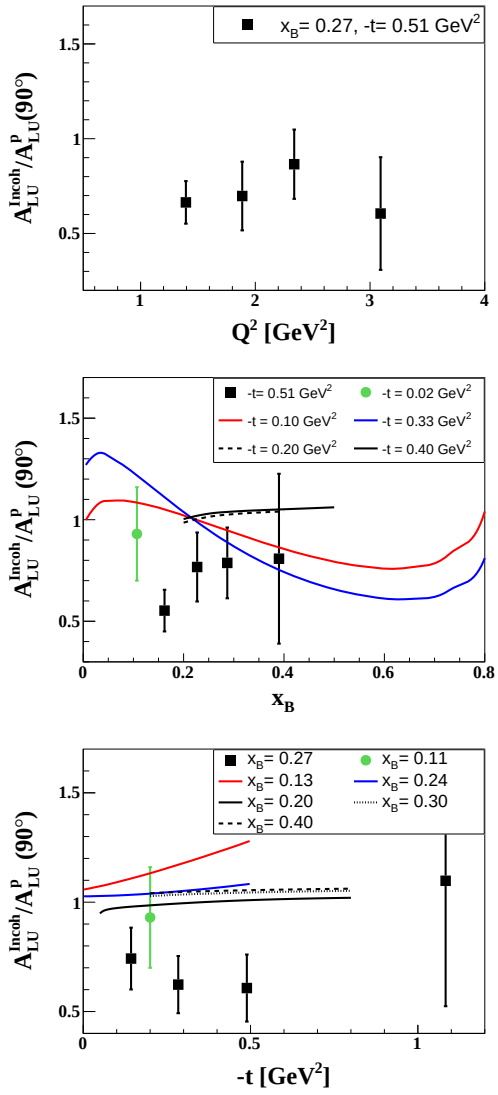

FIG. 6: The A_{LU} ratio of the bound to the free proton at $\phi = 90°$, as a function of Q^2 (top), x_B (middle), and t (bottom). The black squares are from this work, the green circles are the HERMES inclusive measurement [19]. The blue and red curves are results of off-shell calculations [33]. The solid and dashed black curves are from on-shell calculations [35].

fied GPDs as caluclated from the quark-meson coupling model [35]. The off-shell calculations overshoot the data indicating a trend [33]. In particular, the anti-shadowing region seems to be absent in terms of the A_{LU} ratio, while it was predicted by the calculation. Within the given uncertainties, our measured ratios are compatible with the previous measured single point from HERMES [19].

These data, while limited in statistics, proved the experimental feasibility of measuring DVCS of bound-nucleons in addition to the EMC effect within the GPDs framework and led the way to the approval of a next generation nuclear measurements [44]. The future measurements will be carried out using the new CLAS12 spectrometer and the upgraded CEBAF 12 GeV electron beam at an electron-nucleon luminosity of $10^{35}\text{cm}^{-2}\text{s}^{-1}$. The wider accessible phase-space and the higher luminosity will enable us to study nuclear effects and their manifestations on GPDs including the effect of final state interactions.

In summary, we have presented the first exclusive beam-spin asymmetries associated with incoherent DVCS off ^{4}He using an upgraded setup of CLAS spectrometer at Jefferson Lab. Our results were compared to some model calculations based on different assumptions of the nuclear medium effects at the partonic level and allowed us to draw some conclusions. The bound-proton beam-spin asymmetries indicate a suppression compared to the free proton results measured in similar phase-space. While the data are limited in statistics, they opened new insights for extensive future measurements.

The authors acknowledge the staff of the Accelerator and Physics Divisions at the Thomas Jefferson National Accelerator Facility who made this experiment possible. This work was supported in part by the Chilean Comisión Nacional de Investigación Científica y Tecnológica (CONICYT), the Italian Instituto Nazionale di Fisica Nucleare, the French Centre National de la Recherche Scientifique, the French Commissariat à l'Energie Atomique, the U.S. Department of Energy under Contract No. DE-AC02-06CH11357, the United Kingdom Science and Technology Facilities Council (STFC), the Scottish Universities Physics Alliance (SUPA), the National Research Foundation of Korea, and the Office of Research and Economic Development at Mississippi State University. M. Hattawy also acknowledges the support of the Consulat Général de France à Jérusalem. The Southeastern Universities Research Association operates the Thomas Jefferson National Accelerator Facility for the United States Department of Energy under Contract No. DE-AC05-06OR23177.

[1] R. Hofstadter and R. W. McAllister, Phys. Rev. **98**, 217 (1955).
[2] C. F. Perdrisat, V. Punjabi and M. Vanderhaeghen, Prog. Part. Nucl. Phys. **59**, 694 (2007)
[3] Y. L. Dokshitzer, Sov. Phys. JETP **46**, 641 (1977) [Zh. Eksp. Teor. Fiz. **73**, 1216 (1977)].
[4] J. Beringer *et al.* (Particle Data Group), Phys. Rev. D **86**, 010001 (2012).
[5] J. J. Aubert *et al.*, Phys. Lett. vol. B **123**, pp. 275278 (1983).
[6] J. Ashman et al. (EMC Collaboration), Phys. Lett. B **202**, 603 1988.
[7] J. Gomez et al. (SLAC-E139), Phys. Rev. D **49**, 4348 (1994).
[8] A. Airapetian et al. (HERMES Collaboration), Phys. Lett. B **567**, 339 (2003).

[9] J. Seely et al., Phys. Rev. Lett. **103**, 202301 (2009).
[10] J. Arrington et al., Phys. Rev. C **86**, 065204 (2012).
[11] I. Cloët et al., Phys. Rev. Lett. **102**, 252301 (2009).
[12] I. Cloët et al., Phys. Rev. Lett. **109**, 182301 (2012).
[13] D. Mueller, D. Robaschik, B. Geyer, F.M. Dittes, and J. Horejsi, Fortsch. Phys. **42**, 101 (1994).
[14] X.D. Ji, Phys. Rev. Lett. **78**, 610 (1997).
[15] X.D. Ji, Phys. Rev. D **55**, 7114 (1997).
[16] A.V. Radyushkin, Phys. Lett. B **380**, 417 (1996).
[17] A.V. Radyushkin, Phys. Rev. D **56**, 5524 (1997).
[18] S. Stepanyan *et al.* [CLAS Collaboration], Phys. Rev. Lett. **87**, 182002 (2001).
[19] A. Airapetian *et al.* [HERMES Collaboration], Phys. Rev. Lett. **87**, 182001 (2001); JHEP **1207**, 032 (2012); JHEP **1006**, 019 (2010); JHEP **0806**, 066 (2008); Phys. Lett. B **704**, 15 (2011); Phys. Rev. D **75**, 011103 (2007); JHEP **0911**, 083 (2009); Phys. Rev. C **81**, 035202 (2010); JHEP **1210**, 042 (2012).
[20] S. Chekanov *et al.* [ZEUS Collaboration], Phys. Lett. B **573**, 46 (2003).
[21] A. Aktas *et al.* [H1 Collaboration], Eur. Phys. J. C **44**, 1 (2005).
[22] S. Chen *et al.* [CLAS Collaboration], Phys. Rev. Lett. **97**, 072002 (2006).
[23] C. Muñoz Camacho *et al.* [Jefferson Lab Hall A Collaboration], Phys. Rev. Lett. **97**, 262002 (2006).
[24] F.X. Girod *et al.* [CLAS Collaboration], Phys. Rev. Lett. **100**, 162002 (2008).
[25] M. Mazouz *et al.* [Jefferson Lab Hall A Collaboration], Phys. Rev. Lett. **99**, 242501 (2007)
[26] G. Gavalian *et al.* [CLAS Collaboration], Phys. Rev. C **80**, 035206 (2009).
[27] E. Seder *et al.* [CLAS Collaboration], Phys. Rev. Lett. **114**, 032001 (2015).
[28] S. Pisano *et al.* [CLAS Collaboration], Phys. Rev. D **91**, 052014 (2015).
[29] H. S. Jo *et al.* [CLAS Collaboration], Phys. Rev. Lett. **115**, no. 21, 212003 (2015)
[30] J. Seely *et al.*, Phys. Rev. Lett. **103**, 202301 (2009).
[31] R. Dupre, M. Guidal and M. Vanderhaeghen, Phys. Rev. D **95**, no. 1, 011501 (2017)
[32] M. Hattawy *et al.* [CLAS Collaboration], Phys. Rev. Lett. **119**, no. 20, 202004 (2017)
[33] S. Liuti and K. Taneja, Phys. Rev. C **72**, 032201 (2005)
[34] V. Guzey and T. Teckentrup, Phys. Rev. D **74**, 054027 (2006)
[35] V. Guzey, A. W. Thomas and K. Tsushima, Phys. Lett. B **673**, 9 (2009)
[36] J.C. Collins and A. Freund, Phys. Rev. D **59**, 074009 (1999).
[37] X.-D. Ji and J. Osborne, Phys. Rev. D **58**, 094018 (1998).
[38] A. V. Belitsky, D. Mueller and A. Kirchner, Nucl. Phys. B **629**, 323 (2002)
[39] M. Guidal, H. Moutarde, and M. Vanderhaeghen, Rep. Prog. Phys. **76**, 066202 (2013).
[40] K. Hafidi *et al.*, proposal PR-08-024 to JLab PAC33 (unpublished).
[41] B. A. Mecking *et al.* [CLAS Collaboration], Nucl. Instrum. Meth. A **503**, 513 (2003).
[42] R. Dupré *et al.*, arXiv:1706.10160.
[43] M. Hattawy, Ph.D. thesis, Université Paris Sud - Paris XI, France, 2015 [Institution Report No. 2015PA112161].
[44] W. Armstrong *et al.*, arXiv:1708.00888 [nucl-ex]. arXiv:1708.00891 [nucl-ex]. arXiv:1708.00835 [nucl-ex].